M.G. Kozlov, A.V. Reznichenko

EFFECTIVE VERTEX OF QUARK PRODUCTION IN COLLISION OF REGGEIZED QUARK AND GLUON

Effective vertex of quark production
in collision of Reggeized quark and gluon [*]

M. G. Kozlov and A. V. Reznichenko

Budker Institute of Nuclear Physics,
and Novosibirsk State University,
630090 Novosibirsk, Russia

Abstract

We calculated the effective vertex of the quark production in the collision of Reggeized quark and Reggeized gluon in the next-to-leading order (NLO). The vertex in question is the missing component of the multi-Regge NLO amplitudes with the quark and gluon exchanges in t_i channels. The calculation allows us to develop the bootstrap approach to the quark Reggeization proof within next-to-leading logarithmic approximation.

E-mail address: M.G.Kozlov@inp.nsk.su
E-mail address: A.V.Reznichenko@inp.nsk.su

1   Introduction

As it is well known the multi-Regge form of amplitudes at high energies is a base of various theoretical constructions in quantum chromodynamics (QCD) and supersymmetric Yang-Mills theories (SYM). The most famous application of the form resulted in the Balitsky-Fadin-Kuraev-Lipatov (BFKL) [1, 2, 3, 4] approach to the semi-hard processes description in QCD. The simplicity of this form has recently given the powerful tool for various factorization formulae verification in SYM.

Let us now remind the state of art for the Reggeization hypothesis proof. In QCD gluon Reggeization hypothesis (i.e. the multi-Regge form with only gluon exchanges in all t_i channels) was proved in leading logarithmic approximation (LLA) by the authors of the BFKL approach roughly forty years ago. The analyticity and t-channel unitarity were the principal tools of this proof [5]. It proved to be the strong base of the BFKL approach in the leading approximation.

In next-to-leading logarithmic approximation (NLA) we developed the general method based on the compatibility of the hypothetical multi-Regge form of the amplitude with s-channel unitarity [7]. The compatibility is formulated as a series of so-called bootstrap relations which fulfillment ensures validity of the multi-Regge form order by order. The same method turned out to be fruitful in the proof of the multi-Regge form with the quark exchanges in LLA [8]. Then we used the bootstrap approach to prove the NLA gluon Reggeization hypothesis in QCD. The calculation of the quark and gluon one-loop corrections to all bootstrap components gave us possibility to verify all bootstrap relations [9, 10, 11, 12]. Once again our general method was successfully applied to prove NLA gluon Reggeization within supersymmetric Yang-Mills (SYM) theories with arbitrary $\mathcal{N}$ and in the theories with general form of Yukawa interaction [13]. Theoretically our bootstrap approach is applicable for the quark Reggeization NLA proof. But the only unknown component of the NLA amplitude is the Reggeon(G)-Reggeon(Q)-quark one-loop vertex $\gamma_{\mathcal{G}_1 \mathcal{Q}_2}^Q$.

The only missing link of the recurrent bootstrap procedure is the "initial condition". For NLA it is one-loop amplitude with arbitrary leg number n. We supposed these amplitudes to have the correct factorized form cor-

responding to the multi-Regge anzats. It has been verified for small n and should be proved in general.

The main goal of our investigation is to complete the quark Reggeization hypothesis formulation in NLA. For this purpose one should know all effective Reggeon vertices appearing in the multi-Regge form with the quark exchanges up to next-to-leading order. The vertex $\gamma_{\mathcal{G}_1 \mathcal{Q}_2}^{Q}$ in NLO is the final uncalculated component of the amplitude. Another aspect of interest is the construction of the evolution equation kernel in NLO for the Reggeized quark. The vertex $\gamma_{\mathcal{G}_1 \mathcal{Q}_2}^{Q}$ is the final ingredient for the kernel construction. The kernel is of concern since its conformal properties in SYM theory can illuminate the integrability property of this theory and give the connection between different approaches as it occurred for the gluon NLO kernel. Finally, there are some processes (as for instance, recharging processes $p + p \rightarrow n + \Delta^{++}$, $p + \bar{p} \rightarrow n + \bar{n}$ with u- and d- quark exchanges) where the quark exchange amplitude (sub-leading in comparison with the gluon one) might dominantly contribute. Our Reggeon vertices are of some phenomenological interest for these processes.

The article is organized as follows. The second section is devoted to our method explanation and the kinematics description. The third section presents the Reggeization hypothesis, components of our Regge amplitude, and Lorentz and color structures of our one-loop amplitude in the multi-Regge kinematics. In the next section we present the result of our calculation both in fragmentation form reproducing different components of our Regge amplitude and as the full expression. At the end of fourth section we present the resulting expression for the required vertex $\gamma_{\mathcal{G}_1 \mathcal{Q}_2}^{Q}$. In the Appendix we introduce the technique of the loop integration and give the explicit expressions for the master-integrals of our calculation.

2   Amplitude of the quark production in MRK

There are several stages in NLO effective vertex $\gamma_{\mathcal{G}_1 \mathcal{Q}_2}^{Q}$ finding in the next-to-leading order. To calculate this Reggeon vertex we can consider any simple process with the vertex in one-loop approximation. We choose the amplitude $SQ \rightarrow S'Q'\gamma$ of the scalar, quark, and photon production in scalar and quark collision: see Fig. 1. It does not matter for the vertex calculation whether we analyze amplitude in Yang-Mills theory with N_c gluons, with photon, with n_f quarks (in the fundamental color representation), and n_s scalars (in the adjoint representation) or simply QCD amplitude.
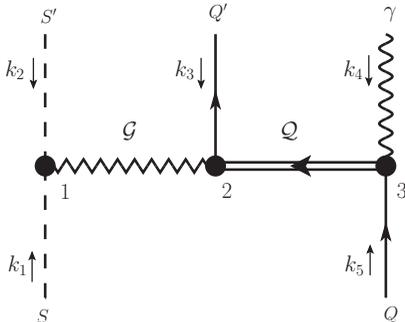
Fig. 1. Regge amplitude of the process $SQ \to S'Q'\gamma$. $\mathcal{G}$ and $\mathcal{Q}$ are Reggeized gluon in t_1-channel and Reggeized quark in t_2-channel respectively. Here blob 1 is the effective vertex $\Gamma^{\mathcal{G}}_{S'S}$, blob 2 — unknown vertex $\gamma^{Q'}_{\mathcal{G}\mathcal{Q}}$, and blob 3 — vertex $\Gamma^{\mathcal{Q}}_{\gamma'Q}$.

We consider all one-loop Feynman diagrams contributing to the process $SQ \to S'Q'\gamma$ at first. There are twenty three different nontrivial one-loop Feynman diagrams: see Fig. 2. There are diagrams labelled according those belonging to pentagons, boxes, triangles and bubble diagram class. First of all we perform the reduction of the amplitude to the master integrals by the "LiteRed"[15] Mathematica package (author R.N. Lee: $www.inp.nsk.su/ \sim lee/programs/LiteRed/$). As a result of the reduction one has pentagon, box, and self-energy nontrivial master integrals. Our master integrals are listed in the Appendix. The method of the tensor integral calculation is presented in Appendix as well. The algorithm of our master integral calculation is presented in Ref. [14]. The next stage is to take Regge limit of the resulting expression for master integrals analytically continued in the physical kinematic region. Finally we compare the result of our calculation with one-loop expression resulting from the hypothetical multi-Regge form [7] of the amplitude in question. In such a way we extract the required vertex.

2.1 Kinematics, color and Lorentz structures of the amplitude

Momentum of the initial scalar S is k_1, of the final scalar S' — k_2, of the final quark Q' produced in the central rapidity region — k_3, of the final photon γ — k_4, and of the initial quark Q — k_5. In Fig. 1 all momenta are considered
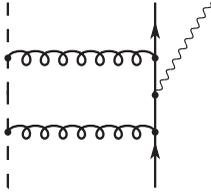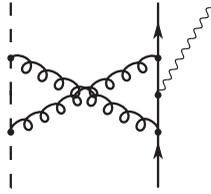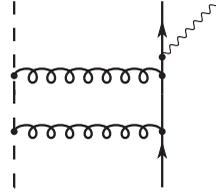
[5]   [5c]   [4.1]
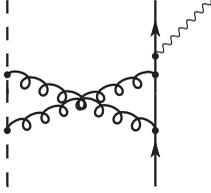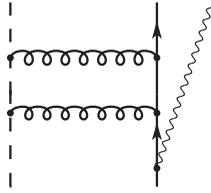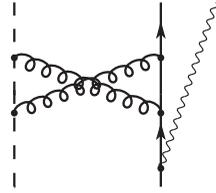
[4.1c]   [4.2]   [4.2c]
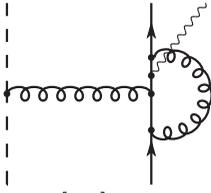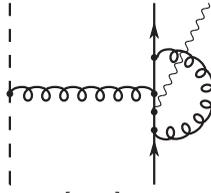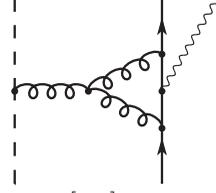
[4.3]   [4.3c]   [4.4]
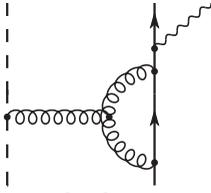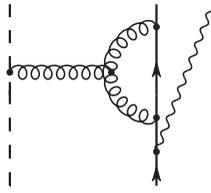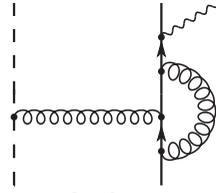
[3.1]   [3.1c]   [3.2]
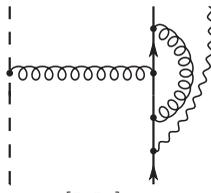
[3.2c]
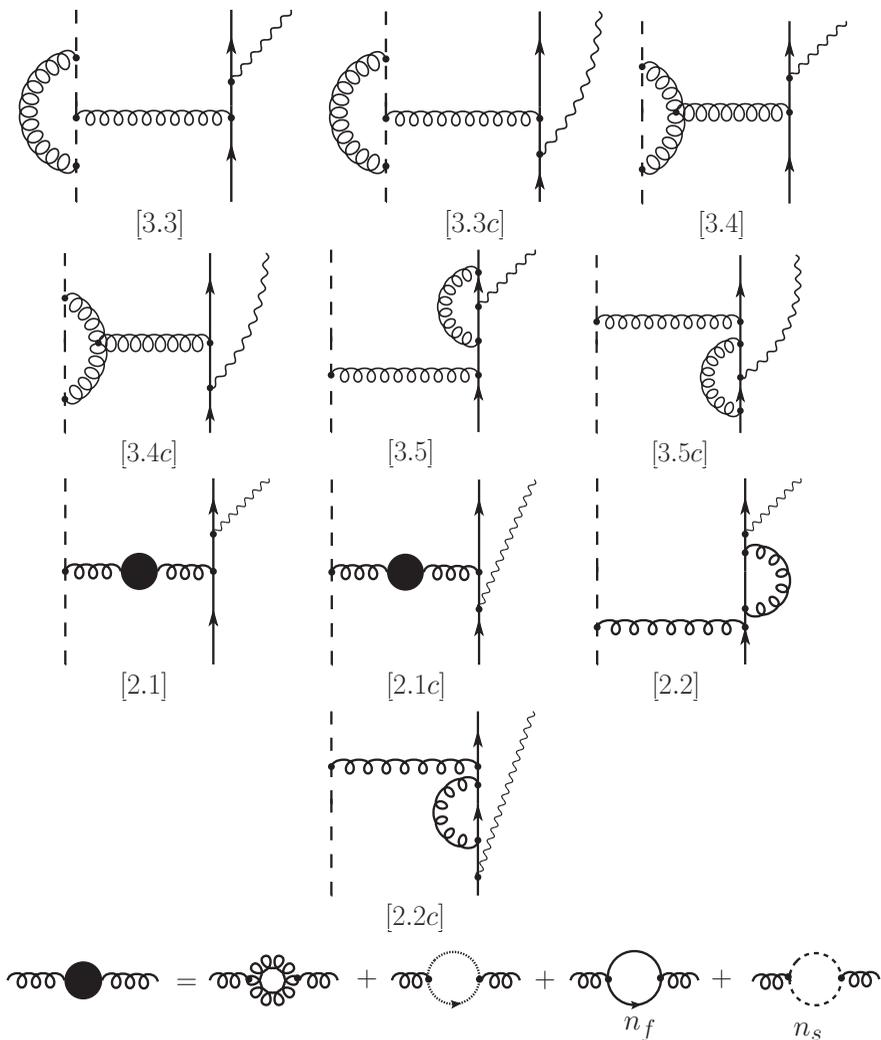
Fig. 2. Nontrivial one-loop diagrams for the process $SQ \to S'Q'\gamma$: pentagons(labelled as [5] and crossed diagrams [5c]), boxes ([4.X] and crossed diagrams [4.Xc]), triangles ([3.X] and crossed diagrams [3.Xc]), and bubbles ([2.X] and crossed diagrams [2.Xc]). The last line is the self-energy insertion with gluons, ghosts, n_f sorts of fermions, and n_s sorts of scalars.

7

to be incoming and light-cone: $k_1 + k_2 + k_3 + k_4 + k_5 = 0$, $k_i^2 = 0$. For the final photon we use the physical gauge with a light cone vector along k_1: $\big(e(k_4), k_4\big) = 0$, $\big(e(k_4), k_1\big) = 0$.

We present Sudakov's decomposition for our momenta with incoming scalar and quark momenta being along light-cone momenta n_1, n_2 ($n_1^2 = 0$, $n_2^2 = 0$, $(n_1, n_2) = 1$): $k_1 = k_1^+ n_1$, $k_i = k_i^+ n_1 + k_i^- n_2 + k_{i\perp}$ for $i = 2, 3, 4$, and $k_5 = k_5^- n_2$. Here n_1, n_2 are light-cone momenta, where $k_i^\pm = (k_i, n_{2,1})$. Here and below the $\perp$ sign is used for components of momenta transverse to n_1, n_2 plane. The scalar productions of particle momenta are expressed through Lorentz invariants:

$$s = 2(k_1, k_5), \ t_1 = 2(k_1, k_2), \ t_2 = 2(k_4, k_5), \ s_1 = 2(k_2, k_3), \ s_2 = 2(k_3, k_4),$$
$$u_1 = 2(k_1, k_3), \ u_2 = 2(k_3, k_5), \ u = 2(k_1, k_4), \ s' = 2(k_2, k_4), \ u' = 2(k_2, k_5). \tag{2.1}$$

And we express the other invariants through independent set: $u_1 = t_2 - t_1 - s_1$, $u_2 = t_1 - t_2 - s_2$, $u = s_1 - t_2 - s$, $s' = s - s_1 - s_2$, $u' = s_2 - t_1 - s$. It is important that the invariants have the following signs in the physical region of our process: $s_1 > 0$, $s_2 > 0$, $s > 0$, $t_1 < 0$, $t_2 < 0$ (and $u_1 < 0$, $u_2 < 0$, $u < 0$, $s' > 0$, $u' < 0$).

The multi-Regge kinematics (MRK) means that we have particles well separated in rapidity space in the final state:

$$k_2^+ \gg k_3^+ \gg k_4^+, \quad k_2^- \ll k_3^- \ll k_4^-. \tag{2.2}$$

Since momenta k_i are on the mass shell one has $k_i^- = -\frac{k_{i\perp}^2}{2k_i^+}$, $i = 2, 3, 4$. We introduce two dimensionless large (in the Regge limit) parameters: $y_1 = k_2^+/k_3^+ \gg 1$ and $y_2 = k_3^+/k_4^+ \gg 1$. In what follows we will use dimensional regularization $D = 4 + 2\epsilon$ taking the limit $\epsilon \to 0$ before the Regge limit. MRK applies also that all transverse momenta are not increasing as $y_i \to \infty$. One can express all of the transverse scalar productions through independent ones ($k_{2\perp}^2$, $k_{3\perp}^2$, $k_{4\perp}^2$): $2(k_2, k_3)_\perp = k_{4\perp}^2 - k_{2\perp}^2 - k_{3\perp}^2$, $2(k_3, k_4)_\perp = k_{2\perp}^2 - k_{3\perp}^2 - k_{2\perp}^2$, and $2(k_2, k_4)_\perp = k_{3\perp}^2 - k_{2\perp}^2 - k_{4\perp}^2$.

Further we consider one-loop amplitude $SQ \to S'Q'\gamma$ as a power function of y_1, y_2 within the accuracy of logarithmic terms (i.e. up to the terms $\ln^k[y_i]$ technically originating from the ϵ decomposition of master integrals). In the Regge limit the leading amplitude behavior is expected to be $\sim y_1\sqrt{y_2}$. Here y_1 comes from Reggeized gluon in the s_1-channel and $\sqrt{y_2}$ — from Reggeized quark in the s_2-channel: see Fig. 1. Our basis bispinor structures (2.4) are proportional to $\sqrt{y_2}$, that is why the order of the multi-Regge limit

calculation for the amplitude is as follows: expansion in $\epsilon \to 0$ with accuracy $\mathcal{O}(\epsilon)$ followed by retaining leading asymptotic power expansion in $y_i \to \infty$.

There are only two independent color structures: "tree" structure $T^a_{S'S}t^a$ and "cross-box" structure $T^a_{S'c}T^b_{cS}t^bt^a$. Here t^a are $SU(N_c)$ quark generators in the fundamental representation, and $T^a_{S'S} = -if^{aS'S}$ are generators of scalars in the adjoint representation. The "tree" structure (i.e. color octet in t_1 channel) turns out to give the leading contribution to the real part of our amplitude. Next, we use the following notation for the Casimir operator:

$$t^a t^a = C_F = \frac{N_c^2 - 1}{2N_c}. \tag{2.3}$$

The amplitude depends not only on the invariants of s_1, s_2, t_1, t_2, s but on the helicity states of the external particles as well.

We assume that external momenta k_i are embedded in a four-dimensional subspace of the momentum space with $D = 4 + 2\epsilon$ dimensions, while the photon polarization is D-vector. In that case there are six independent Lorentz helicity structures:

$$\bar{u}(k_3)\not{e}u(k_5)\,,\ \bar{u}(k_3)\not{k}_1\not{k}_4\not{e}u(k_5)\,,\ (e, k_2)\bar{u}(k_3)\not{k}_1 u(k_5)\,,\ (e, k_2)\bar{u}(k_3)\not{k}_4 u(k_5)\,,$$
$$(e, k_3)\bar{u}(k_3)\not{k}_1 u(k_5)\,,\ (e, k_3)\bar{u}(k_3)\not{k}_4 u(k_5)\,. \tag{2.4}$$

In the multi-Regge kinematics we can choose the following independent structures with only transverse $(D-2)$ components involved:

$$\bar{u}(k_3)\not{e}_\perp u(k_5)\,,\ \bar{u}(k_3)\not{k}_{2\perp}\not{k}_{4\perp}\not{e}_\perp u(k_5)\,, (e, k_2)_\perp\bar{u}(k_3)\not{k}_{2\perp}u(k_5)\,,$$
$$(e, k_2)_\perp\bar{u}(k_3)\not{k}_{4\perp}u(k_5)\,, (e, k_4)_\perp\bar{u}(k_3)\not{k}_{2\perp}u(k_5)\,, (e, k_4)_\perp\bar{u}(k_3)\not{k}_{4\perp}u(k_5)\,. \tag{2.5}$$

In the limit $D \to 4$ the first two structures become dependent since one can express $\not{e}_\perp$ in terms of $\not{k}_{2\perp}$, $\not{k}_{4\perp}$:

$$e^\mu_\perp = k^\mu_{2\perp} \frac{k^2_{4\perp}(e, k_2)_\perp - (k_2, k_4)_\perp(e, k_4)_\perp}{k^2_{2\perp}k^2_{4\perp} - (k_2, k_4)^2_\perp} + $$
$$+ k^\mu_{4\perp} \frac{-(k_2, k_4)_\perp(e, k_2)_\perp + k^2_{2\perp}(e, k_4)_\perp}{k^2_{2\perp}k^2_{4\perp} - (k_2, k_4)^2_\perp}. \tag{2.6}$$

This means that the part of metric tensor $g^{\mu\nu}_{D-4} \sim \mathcal{O}(\epsilon)$ vanishes in the dimensional limit $D \to 4$.

3 Regge amplitude structure

According to the hypothesis of the quark and gluon Reggeization in NLA the real part of the amplitude $A + B \rightarrow A' + J_1 + \cdots + J_n + B'$ in the MRK has the form

$$\Re\mathcal{A}_{2 \rightarrow n+2} = \bar{\Gamma}_{A'A}^{R_1} \left(\mathcal{P} \prod_{i=1}^{n} e^{\omega_{R_i}(q_i)(z_{i-1}-z_i)} \widehat{D}_{R_i} \gamma_{R_i R_{i+1}}^{J_i} \right) \times$$

$$\times \, e^{\omega_{R_{n+1}}(q_{n+1})(z_n - z_{n+1})} \widehat{D}_{R_{n+1}} \Gamma_{B'B}^{R_{n+1}} \, , \tag{3.1}$$

where $\mathcal{P} \prod$ is the product ordered along the fermion line. We use the notation

$$\widehat{D}_{R_i} = \begin{cases} \dfrac{1}{q_{i\perp}^2} \, , & R_i = \mathcal{G}_i, \\[2mm] -\dfrac{\slashed{q}_{i\perp}}{q_{i\perp}^2} \, , & R_i = \mathcal{Q}_i, \end{cases} \tag{3.2}$$

for the Reggeon R_i (gluon or quark) propagator. Then $z_i = \frac{1}{2} \ln \frac{k_i^+}{k_i^-}$ are rapidities of the final jets J_i. In next-to-leading logarithmic approximation (NLA) jets J_i are either one parton or the partons couple with close rapidities. Lastly, $\omega_R(q)$ in (3.1) is the Regge trajectory of the Reggeon R (gluon or quark) with momentum q.

There are several effective vertices ($\bar{\Gamma}_{A'A}^{R_1}$, $\Gamma_{B'B}^{R_{n+1}}$) for the particle–jet transition in the "fragmentation" kinematic region. As for particle–particle transition (pure multi-Regge kinematics) one has the following vertices in QCD:

$$\Gamma_{G'G}^{\mathcal{G}} \, , \, \Gamma_{Q'Q}^{\mathcal{G}} \, , \, \Gamma_{G'Q}^{\mathcal{Q}}.$$

There is an extra vertex $\Gamma_{S'S}^{\mathcal{G}}$ for SYM. All these vertices are calculated within the NLO [16] (for SYM case see [13]). The vertex the quark-photon transition $\Gamma_{\gamma'Q}^{Q_2}$ may be found in [16] as well. For quasi-multi-Regge kinematics (QMRK) case of particle–couple transition one has in QCD:

$$\Gamma_{\{G_1G_2\}G}^{\mathcal{G}} \, , \, \Gamma_{\{Q_1Q_2\}G}^{\mathcal{G}} \, , \, \Gamma_{\{G_1Q_2\}Q}^{\mathcal{G}} \, , \, \Gamma_{\{G_1G_2\}Q}^{\mathcal{Q}} \, , \, \Gamma_{\{G_1Q_2\}G}^{\mathcal{Q}} \, , \, \Gamma_{\{Q_1Q_2\}Q}^{\mathcal{Q}}.$$

All these vertices are known: see [17, 18]. For SYM there are some additional vertices ($\Gamma_{\{S_1S_2\}G}^{\mathcal{G}}$, $\Gamma_{\{GS'\}S}^{\mathcal{G}}$, $\Gamma_{\{Q_1Q_2\}S}^{\mathcal{G}}$, $\Gamma_{\{Q'S\}Q}^{\mathcal{G}}$): the corresponding calculation one can find in Ref. [13].

There are several effective vertices ($\gamma_{R_i R_{i+1}}^{J_i}$) for the jet production in Reggeon-Reggeon collision in the central region of rapidity. For one-particle production we have QCD vertices

$$\gamma_{\mathcal{G}_1 \mathcal{G}_2}^G \, , \ \gamma_{\mathcal{Q}_1 \mathcal{Q}_2}^G \, , \ \gamma_{\mathcal{Q}_1 \mathcal{G}_2}^Q \, .$$

Vertices $\gamma_{\mathcal{G}_1 \mathcal{G}_2}^G$, $\gamma_{\mathcal{Q}_1 \mathcal{Q}_2}^G$ were calculated in NLO [21, 22, 23, 6]. Effective vertex $\gamma_{\mathcal{Q}_1 \mathcal{G}_2}^Q$ was calculated in the leading order only. Our purpose is to find one-loop corrections to it. Vertices for couple production (QMRK) in the central region of rapidity

$$\gamma_{\mathcal{G}_1 \mathcal{G}_2}^{\{G_1 G_2\}} \, , \ \gamma_{\mathcal{G}_1 \mathcal{G}_2}^{\{Q_1 Q_2\}} \, , \ \gamma_{\mathcal{Q}_1 \mathcal{G}_2}^{\{Q_1 G_2\}} \, , \ \gamma_{\mathcal{Q}_1 \mathcal{Q}_2}^{\{G_1 G_2\}} \, , \ \gamma_{\mathcal{Q}_1 \mathcal{Q}_2}^{\{Q_1 Q_2\}}$$

are calculated in QCD with required NLO accuracy [17, 18] as well. In SYM one has an extra vertex $\gamma_{R_1 R_2}^{\{S_1 S_2\}}$ that was calculated some years ago [19].

Note that QMRK is sub-leading kinematic i.e. all necessary vertices are on the tree level. For QMRK amplitudes with gluon and quark exchanges the Reggeization hypothesis was proved in [20].

In the following we will use the standard momentum notations for the Regge amplitude $SQ \to S'Q'\gamma$ (see Fig. 1):

$$q_{1\perp} \equiv (k_2 + k_1)_\perp = k_{2\perp}, \ q_{2\perp} \equiv (-k_4 - k_5)_\perp = -k_{4\perp}, \ k_\perp \equiv -k_{3\perp}, \quad (3.3)$$

with k being momentum of the quark produced. According to the hypothesis of the quark and gluon Reggeization in NLA (3.1), the real part of the amplitude $SQ \to S'Q'\gamma$ in the multi-Regge kinematics reads as

$$\Re \mathcal{A}_8 = \Gamma_{S'S}^{R_1} \left(\frac{s_1}{\sqrt{q_{1\perp}^2 k_\perp^2}} \right)^{\omega_g(q_1)} \frac{1}{q_{1\perp}^2} \gamma_{R_1 Q_2}^Q \left(\frac{s_2}{\sqrt{k_\perp^2 q_{2\perp}^2}} \right)^{\omega_q(q_2)} \left[-\frac{\slashed{q}_{2\perp}}{q_{2\perp}^2} \right] \Gamma_{\gamma'Q}^{Q_2}.$$

$$(3.4)$$

3.1 Regge trajectories and effective vertices

Now we present an expression for the one-loop trajectories of a quark and gluon:

$$\omega_q(q) = -2C_F g^2(-ia_\Gamma) \frac{(-q_\perp^2)^\epsilon}{\epsilon} \, , \ \omega_g(q) = -2N_c g^2(-ia_\Gamma) \frac{(-q_\perp^2)^\epsilon}{\epsilon}. \quad (3.5)$$

The constant a_Γ emerges from the integrals as a common factor (6.8). The combination of $N_c g^2(-ia_\Gamma)$ will arise often and it relates with $\bar{g}^2$ notation as

follows:

$$N_c g^2 (-ia_\Gamma) \equiv N_c g^2 \frac{\Gamma(1-\epsilon)}{(4\pi)^{2+\epsilon}} \frac{\Gamma^2(1+\epsilon)}{\Gamma(1+2\epsilon)} = \bar{g}^2 \left(1 - \frac{\pi^2}{6}\epsilon^2 + \mathcal{O}(\epsilon^3)\right). \quad (3.6)$$

Now we present the scalar to scalar Regge vertex in the following way [13]:

$$\Gamma^{R_1}_{S'S} = 2k_1^+ g T^{R_1}_{S'S} (1 + \delta_S), \quad \delta_S = \delta_S^c + \delta_S^{s.e.} + \delta_S^v + \delta_S^A. \quad (3.7)$$

Expressions for the corrections (δ's) to vertex of the scalar scattering can be found in [13] (there are corrections in the framework of supersymmetric Yang–Mills theory, but the QCD result can be obtained easily):

$$\delta_S^A + \delta_S^c = (-ia_\Gamma) g^2 N_c (-q_{1\perp}^2)^\epsilon \left(-\frac{5}{4\epsilon^2} + \frac{1}{2\epsilon} - 1 + \frac{\pi^2}{2} \right), \quad (3.8)$$

$$\delta_S^{s.e.} = (-ia_\Gamma) N_c g^2 \frac{(-q_{1\perp}^2)^\epsilon}{\epsilon} \left(-\left[\frac{5}{6} - \frac{31}{18}\epsilon\right] + n_s \left[\frac{1}{12} - \frac{2}{9}\epsilon\right] + \frac{n_f}{N_c}\left[\frac{1}{3} - \frac{5}{9}\epsilon\right] \right), \quad (3.9)$$

$$\delta_S^v = (-ia_\Gamma) N_c g^2 \frac{(-q_{1\perp}^2)^\epsilon}{\epsilon^2} \left(\left[\frac{5}{4} - \frac{3}{2}\epsilon + 3\epsilon^2\right] + \left[-2 + 4\epsilon - 8\epsilon^2\right] \right). \quad (3.10)$$

Here the superscript c denotes the universal contribution from the central rapidity region, the index $s.e.$ denotes the contribution of the mass (self-energy) operator, the index v denotes the contribution of the vertex corrections, and the index A represents the contribution coming from the rapidity close to the initial particle. All corrections are presented in ϵ decomposition with required accuracy.

Corrections to vertex of photon production is more complicated since the structure contains helicity violating terms:

$$\Gamma^{Q_2}_{\gamma'Q} = -e\left(\slashed{\epsilon}_\perp + \slashed{\epsilon}_\perp \delta_{1\gamma} + \frac{(eq_2)_\perp}{q_{2\perp}^2}\slashed{q}_{2\perp}\delta_{2\gamma}\right)u(k_5), \quad (3.11)$$

$$\delta_{1\gamma} = \delta_{1\gamma}^{s.e.} + \delta_{1\gamma}^v + \delta_{1\gamma}^A + \delta_{1\gamma}^c, \quad \delta_{2\gamma} = \delta_{2\gamma}^v + \delta_{2\gamma}^A. \quad (3.12)$$

Expression for these corrections can be found in [16]:

$$\delta_{1\gamma}^A + \delta_{1\gamma}^c = g^2(-ia_\Gamma)(-q_{2\perp}^2)^\epsilon(-C_F)\left[\frac{1}{\epsilon^2} - \frac{\pi^2}{2}\right], \quad (3.13)$$

$$\delta_{1\gamma}^v = C_F g^2(-ia_\Gamma)(-q_{2\perp}^2)^\epsilon \frac{1 - 4\epsilon}{\epsilon}, \quad (3.14)$$

$$\delta_{1\gamma}^{s.e.} = C_F g^2(-ia_\Gamma)(-q_{2\perp}^2)^\epsilon \frac{1-\epsilon}{2\epsilon}, \tag{3.15}$$

$$\delta_{2\gamma}^v = C_F g^2(-ia_\Gamma)(-q_{2\perp}^2)^\epsilon \frac{(-2)(2-5\epsilon)}{\epsilon}, \tag{3.16}$$

$$\delta_{2\gamma}^A = C_F g^2(-ia_\Gamma)(-q_{2\perp}^2)^\epsilon \frac{4(1-2\epsilon)}{\epsilon}. \tag{3.17}$$

We parametrize the unknown vertex of quark production in quark-Reggeon collision as

$$\gamma_{R_1 Q_2}^Q = -g\frac{1}{k_3^+}\bar{u}(k_3)t^{R_1}\left(\slashed{q}_{1\perp} + \slashed{q}_{1\perp}\delta_{1Q} + \slashed{q}_{2\perp}\delta_{2Q}\right). \tag{3.18}$$

The term δ_{1Q} is a correction to leading order structure. The correction δ_{2Q} stands before the structure, that is absent in the leading order (the mass operator corrections contribute only in the δ_{1Q} coefficient):

$$\delta_{1Q} = \delta_{1Q}^{s.e.1} + \delta_{1Q}^{s.e.2} + \delta_{1Q}^{v,c}, \quad \delta_{2Q} = \delta_{2Q}^{v,c}. \tag{3.19}$$

3.2 Lorentz and color structures of the Regge amplitude

Now we consider the real part of the amplitude in question.

In the first place we will be interested in octet color, or "tree", structure coefficient of Regge amplitude obtained in our calculation after the Regge limit procedure.

Let us introduce the notation for the basic Lorentz structures of our Regge amplitude. There is only one Born structure

$$A^{Born} = -2y_1 g^2 e T_{S'S}^{R_1} \frac{\bar{u}(k_3)t^{R_1}\slashed{q}_{1\perp}\slashed{q}_{2\perp}\slashed{\epsilon}_\perp u(k_5)}{q_{1\perp}^2 q_{2\perp}^2}. \tag{3.20}$$

The next structure A_8^e arises from the correction to the Regge vertex for quark production in the central region and violates the helicity

$$A_8^e = -2y_1 g^2 e T_{S'S}^{R_1} \frac{\bar{u}(k_3)t^{R_1}\slashed{\epsilon}_\perp u(k_5)}{q_{1\perp}^2}. \tag{3.21}$$

Structure $A_8^{q_1}$ arises from correction to the Regge vertex for quark-photon transition and violates the helicity as well

$$A_8^{q_1} = -2y_1 g^2 e T_{S'S}^{R_1} \frac{\bar{u}(k_3)t^{R_1}\slashed{q}_{1\perp} u(k_5)(e,q_2)_\perp}{q_{1\perp}^2 q_{2\perp}^2}. \tag{3.22}$$

13

The final structure that appears after the Regge limit in our calculations is as follows

$$A_8^{q_2} = -2y_1 g^2 e T_{S'S}^{R_1} \frac{\bar{u}(k_3) t^{R_1} \not{q}_{2\perp} u(k_5)(e, q_2)_\perp}{q_{1\perp}^2 q_{2\perp}^2}. \qquad (3.23)$$

Decomposition of the multi-Regge form of the amplitude $SQ \to S'Q'\gamma$ (3.4) in the coupling constant up to the next-to-leading order gives us:

$$\Re \mathcal{A}_8 = A^{Born} \Big(1 + \omega_g(q_1) \ln y_1 + \omega_q(q_2) \ln y_2 + \frac{\omega_g(q_1)}{2} \ln \Big[\frac{k_\perp^2}{q_{1\perp}^2}\Big] +$$
$$+ \frac{\omega_q(q_2)}{2} \ln \Big[\frac{q_{2\perp}^2}{k_\perp^2}\Big] \delta_S + \delta_{1Q} + \delta_{1\gamma} \Big) + A_8^e \delta_{2Q} + A_8^{q_1} \delta_{2\gamma} + \mathcal{O}(eg^6). \qquad (3.24)$$

If we calculate the one-loop corrections for $SQ \to S'Q'\gamma$ amplitude and substract the known corrections for the effective vertices $\Gamma_{S'S}^{\mathcal{G}}$, $\Gamma_{\gamma Q}^{\mathcal{Q}}$ and the terms with Regge trajectories contribution, then we obtain the corrections for effective vertex $\gamma_{\mathcal{G}Q}^Q$.

4   Result of the amplitude $SQ \to S'Q'\gamma$ calculation

Let us present the result of the calculation procedure described at the beginning of Section 2. Here we give the calculation result in the Regge limit and group diagrams into the expressions with specific elements for the Regge amplitude. We use notations (3.20)–(3.23) for structures from the previous Section and the notation (6.8) for the common factor a_Γ.

Now we present characteristic diagram contributions reproducing different components of the Regge amplitude: photon and scalar vertex corrections, Regge trajectories, and the corrections to the unknown vertex.

The sum of diagrams giving the correction to the photon vertex reads as

$$\Re\big(A_{3.5} + A_{3.5c}\big) =$$

$$= g^2(-ia_\Gamma) C_F \Big\{ -A_8^e \ln y_2 - (-q_{2\perp}^2)^\epsilon \frac{1}{\epsilon} \Big[2(2-5\epsilon)\big(A_8^{q_1}+A_8^{q_2}\big) - (1-4\epsilon) A^{Born} \Big] \Big\}. \qquad (4.1)$$

It is easy to see that these diagrams (3.5 group) contain the large logarithm $\ln y_2$. Diagrams describing the mass operator of the quark in the t_2-channel contain $\ln y_2$ as well:

$$\Re\big(A_{2.2} + A_{2.2c}\big) = g^2(-ia_\Gamma)\, C_F\left(A^{Born}\frac{1-\epsilon}{\epsilon}(-q_{2\perp}^2)^\epsilon - A_e^8\ln y_2\right). \quad (4.2)$$

Diagrams of the vacuum polarization of the gluon in the t_1-channel result in the expression (in $\epsilon \to 0$ decomposition)

$$A_{2.1X} = N_c g^2(-ia_\Gamma) A^{Born}\frac{(-q_{1\perp}^2)^\epsilon}{\epsilon}\times$$
$$\times\left(-\left(\frac{5}{3}-\frac{31}{9}\epsilon\right) + \frac{n_s}{2}\left(\frac{1}{3}-\frac{8}{9}\epsilon\right) + \frac{n_f}{N_c}\left(\frac{2}{3}-\frac{10}{9}\epsilon\right)\right). \quad (4.3)$$

The following group of diagrams gives the correction to the scalar vertex:

$$A_{3.3} + A_{3.3c} + A_{3.4} + A_{3.4c} = N_c g^2(-ia_\Gamma) A^{Born}\frac{(-q_{1\perp}^2)^\epsilon}{\epsilon^2}\times$$
$$\times\left(-(2-4\epsilon+8\epsilon^2) + \frac{1}{4}(5-6\epsilon+12\epsilon^2)\right). \quad (4.4)$$

Diagrams describing Reggeization of quarks and gluons (i.e. yielding the Regge trajectories) and delivering the correction to the vertex of the quark production in the central region give the following real part for the octet (tree) color structure:

$$\Re\big(A_5 + A_{4.1} + A_{4.2} + A_{4.3} + A_{4.3c} + A_{4.4} + A_{3.1} + A_{3.1c} + A_{3.2} + A_{3.2c}\big)\Big|_8 =$$

$$= -ig^2 a_\Gamma\Bigg\{ A_8^e\Bigg[(N_c - C_F)\left(1 + \frac{k_\perp^2}{q_{1\perp}^2 - q_{2\perp}^2} - \frac{q_{1\perp}^2 k_\perp^2}{(q_{1\perp}^2 - q_{2\perp}^2)^2}\ln\left[\frac{q_{1\perp}^2}{q_{2\perp}^2}\right]\right) +$$

$$+ C_F\left(\frac{3q_{1\perp}^2}{q_{1\perp}^2 - q_{2\perp}^2}\ln\left[\frac{q_{1\perp}^2}{q_{2\perp}^2}\right] + 2\ln y_2\right)\Bigg] + A^{Born}\Bigg[C_F\left(-\frac{2-\epsilon}{\epsilon^2}(-q_{2\perp}^2)^\epsilon -\right.$$

$$\left. -\frac{2}{\epsilon}(-q_{2\perp}^2)^\epsilon\ln y_2 + \frac{2\pi^2}{3} - 4 + \frac{3q_{1\perp}^2}{q_{1\perp}^2 - q_{2\perp}^2}\ln\left[\frac{q_{1\perp}^2}{q_{2\perp}^2}\right] + 2\text{Li}_2\left[1 - \frac{q_{1\perp}^2}{q_{2\perp}^2}\right]\right) -$$

$$- N_c\left(\frac{1}{\epsilon^2}(-k_\perp^2)^\epsilon + \frac{2}{\epsilon}(-q_{1\perp}^2)^\epsilon\ln y_1 + \frac{1+2\epsilon}{4\epsilon^2}(-q_{1\perp}^2)^\epsilon - \frac{2\pi^2}{3} - 2 +\right.$$

$$\left.+\ln\left[\frac{q_{1\perp}^2}{q_{2\perp}^2}\right]\ln\left[\frac{k_\perp^2}{q_{2\perp}^2}\right] + 2\text{Li}_2\left[1 - \frac{q_{1\perp}^2}{q_{2\perp}^2}\right]\right)\Bigg] + A_8^{q_1}\left[4C_F\frac{1-2\epsilon}{\epsilon}(-q_{2\perp}^2)^\epsilon\right] +$$

$$+ A_8^{q_2}\left[2C_F\frac{2-5\epsilon}{\epsilon}(-q_{2\perp}^2)^\epsilon\right]\Bigg\}. $$
$$(4.5)$$

Corrections to Regge vertices

Contribution to the mass operator in the t_1-channel comes from diagrams $A_{2.1}$ и $A_{2.1c}$.

$$A_{2.1} + A_{2.1c} = 2\delta_S^{s.e.} A^{Born} = 2\delta_{1Q}^{s.e.1} A^{Born}. \tag{4.6}$$

Non-logarithmic part of diagrams $A_{2.2}$ and $A_{2.2c}$ (the large logarithm $\ln y_2$ presents in the diagram $A_{2.2}$) contributes to the mass operator in the t_2-channel resulting in

$$\Re(A_{2.2} + A_{2.2c})\Big|_{(\ln y_2)^0} = 2\delta_{1Q}^{s.e.2} A^{Born} = 2\delta_{1\gamma}^{s.e.} A^{Born}. \tag{4.7}$$

The sum of the diagrams $3.3X$ and $3.4X$ contributes to the correction δ_S^v:

$$A_{3.3} + A_{3.3c} + A_{3.4} + A_{3.4c} = A^{Born}\delta_S^v. \tag{4.8}$$

The sum of the box-type diagrams in the t_1-channel with large logarithms has only the tree color structure (octet in t_1-channel) and yields the gluon trajectory

$$(A_{4.1} + A_{4.2} + A_{4.1c} + A_{4.2c})\Big|_{\ln y_1} = A^{Born}\omega_g(q_1)\ln y_1. \tag{4.9}$$

In the cross-box color structure the large logarithm $\ln y_1$ cancels completely (according to the gluon Reggeization).

For t_2-channel expression before the large logarithm $\ln y_2$ is reduced to the quark trajectory by more complex way than in t_1-channel:

$$(A_{4.3} + A_{4.3c} + A_{4.4} + A_{3.1} + A_{3.2} + A_{3.5} + A_{2.2})\Big|_{\ln y_2} = A^{Born}\omega_q(q_2)\ln y_2. \tag{4.10}$$

Squares of large logarithms $\ln y_2$ cancel in the following sums:

$$(A_{4.3} + A_{4.3c})\Big|_{(\ln y_2)^2} = 0, \quad (A_{4.4} + A_{3.1})\Big|_{(\ln y_2)^2} = 0. \tag{4.11}$$

The following real part of the octet (tree) color structure gives almost full contribution to the correction to the Regge vertex $\gamma_{R_1 Q_2}^Q$.

$$Re(A_{4.3} + A_{4.3c} + A_{4.4} + A_{3.1} + A_{3.1c} + A_{3.2} + A_{3.2c} + A_5 + A_{4.1} + A_{4.2})\Big|_8 =$$

$$= A^{Born}\left(\omega_g(q_1)\left[\ln y_1 + \frac{1}{2}\ln\frac{k_\perp^2}{q_{1\perp}^2}\right] + \omega_q(q_2)\left[\ln y_2 + \frac{1}{2}\ln\frac{q_{2\perp}^2}{k_\perp^2}\right] + \right.$$

16

$$+\delta_{1Q}^{v,c} + \delta_{1\gamma}^A + \delta_{1\gamma}^c + \delta_S^c + \delta_S^A \Bigg) + A_8^e\delta_{2Q} + A_8^{q_1}\delta_{2\gamma}^c - A_8^{q_2}\delta_{3\gamma}. \qquad (4.12)$$

Together with the mass operator contribution (4.6) and (4.7) one obtain the full result for the vertex in question. In the sum (4.12) there are some contributions to the Regge vertices in the fragmentation region, i.e. $\Gamma_{S'S}^{R_1}$ — see (3.7) and $\Gamma_{\gamma'Q}^{Q_2}$ — see (3.11), and the contributions to the Regge trajectories.

The vertex correction to the photon production vertex comes from the following diagram group and reads:

$$\Re(A_{3.5} + A_{3.5c})\Big|_{(\ln y_2)^0} = A^{Born}\delta_{1\gamma}^v + A_8^{q_1}\delta_{2\gamma}^v + A_8^{q_2}\delta_{3\gamma}. \qquad (4.13)$$

It is obvious from expressions (4.12) and (4.13) that the structure of $A_8^{q_2}$ cancels in the final expression for the Regge amplitude.

The cross-box color structure and the imaginary part of the amplitude

The cross-box color structure presents only in the diagrams: $5X, 4.1X, 4.2X$. We introduce the notation for the basic structure, which is contained in the cross-box color structure:

$$A_{c-b} = -2y_1 g^2 e T_{S'c}^a T_{cS}^b \frac{\bar{u}(k_3)t^b t^a \slashed{q}_{1\perp}\slashed{q}_{2\perp}\slashed{\epsilon}_\perp u(k_5)}{q_{1\perp}^2 q_{2\perp}^2}. \qquad (4.14)$$

The cross-box color structure is derived from the amplitude resulting in:

$$\mathcal{A}\Big|_{crossbox} = g^2(-ia_\Gamma)A_{c-b}(-i\pi)\frac{4}{\epsilon}(-q_{1\perp}^2)^\epsilon. \qquad (4.15)$$

The imaginary part of the amplitude contains tree and cross-box color structures:

$$\Im\mathcal{A} = \pi\frac{(-ia_\Gamma)g^2}{\epsilon}\left[N_c A^{Born}\left((-q_{1\perp}^2)^\epsilon + (-k_\perp^2)^\epsilon\right) - A_{c-b}4(-q_{1\perp}^2)^\epsilon\right]. \qquad (4.16)$$

It is easy to see that the imaginary part does not contain large logarithms ($\ln y_1$ and $\ln y_2$) at all as it must be according to the Reggeization hypothesis.

The final result for the amplitude and the vertex $\gamma^Q_{R_1 Q_2}$

Now we present the resulting expression for one-loop corrections to $SQ \to S'Q'\gamma$ amplitude in the MRK with $\mathcal{O}(\epsilon)$ accuracy:

$$
i\mathcal{A} = a_\Gamma g^2 A^{Born} \Bigg\{ C_F (-q^2_{2\perp})^\epsilon \left(-\frac{2}{\epsilon^2} + \frac{3}{\epsilon} - 9 - \frac{2}{\epsilon} \ln y_2 + \frac{2\pi^2}{3} + \right.
$$

$$
\left. + \frac{3q^2_{1\perp}}{q^2_{1\perp} - q^2_{2\perp}} \ln \left[\frac{q^2_{1\perp}}{q^2_{2\perp}} \right] + 2\mathrm{Li}_2 \left[1 - \frac{q^2_{1\perp}}{q^2_{2\perp}} \right] \right) + N_c (-q^2_{1\perp})^\epsilon \times
$$

$$
\times \left(-\frac{2}{\epsilon^2} + \frac{1}{\epsilon} \left(\frac{1}{3} + \frac{4}{9}\epsilon + n_s \left(\frac{1}{6} - \frac{4}{9}\epsilon \right) + \frac{n_f}{N_c} \left(\frac{2}{3} - \frac{10}{9}\epsilon \right) + \ln \left[\frac{q^2_{1\perp}}{k^2_\perp} \right] - 2\ln y_1 \right) -
$$

$$
- \frac{1}{2} \ln^2 \left[\frac{q^2_{1\perp}}{k^2_\perp} \right] + \frac{2\pi^2}{3} - \ln \left[\frac{q^2_{1\perp}}{q^2_{2\perp}} \right] \ln \left[\frac{k^2_\perp}{q^2_{2\perp}} \right] - 2\mathrm{Li}_2 \left[1 - \frac{q^2_{1\perp}}{q^2_{2\perp}} \right] \right) \Bigg\} + 2C_F a_\Gamma g^2 A^{q_1}_8 +
$$

$$
+ a_\Gamma g^2 A^e_8 \Bigg\{ (N_c - C_F) \left(1 + \frac{k^2_\perp}{q^2_{1\perp} - q^2_{2\perp}} - \frac{q^2_{1\perp} k^2_\perp}{(q^2_{1\perp} - q^2_{2\perp})^2} \ln \left[\frac{q^2_{1\perp}}{q^2_{2\perp}} \right] \right) +
$$

$$
+ C_F \frac{3\, q^2_{1\perp}}{q^2_{1\perp} - q^2_{2\perp}} \ln \left[\frac{q^2_{1\perp}}{q^2_{2\perp}} \right] \Bigg\} +
$$

$$
+ i\pi \frac{a_\Gamma g^2}{\epsilon} \Bigg\{ N_c A^{Born} \left((-q^2_{1\perp})^\epsilon + (-k^2_\perp)^\epsilon \right) - A_{c-b} 4 (-q^2_{1\perp})^\epsilon \Bigg\}.
$$

$$
(4.17)
$$

It is easy to see that the coefficients before structures $A^{q_1}_8$, A^e_8 are finite in the limit $D \to 4$.

Comparing the result (4.17) of the amplitude calculation with the expression (3.24) for the real part coming from the Reggeization hypothesis we can present the effective Regge vertex of the quark production in the central rapidity region in the NLO:

$$
\gamma^Q_{R_1 Q_2} = -g \frac{1}{k^+_3} \bar{u}(k_3) t^{R_1} \left(\slashed{q}_{1\perp} + \slashed{q}_{1\perp} \delta_{1Q} + \slashed{q}_{2\perp} \delta_{2Q} \right),
$$

where

$$
\delta_{1Q} = \delta^{s.e.1}_{1Q} + \delta^{s.e.2}_{1Q} + \delta^{v,c}_{1Q}.
$$

Contribution from mass operator has the form:

$$\delta_{1Q}^{s.e.1} + \delta_{1Q}^{s.e.2} = \frac{N_c g^2(-ia_\Gamma)}{2}\left\{(-q_{1\perp}^2)^\epsilon\left[\frac{n_s}{2}\left(\frac{1}{3\epsilon} - \frac{8}{9}\right) - \left(\frac{5}{3\epsilon} - \frac{31}{9}\right) + \right.\right.$$

$$\left.\left. + \frac{n_f}{N_c}\left(\frac{4}{3\epsilon} - \frac{20}{9}\right)\right] + (-q_{2\perp}^2)^\epsilon\frac{C_F}{N_c}\left(\frac{1}{\epsilon} - 1\right)\right\}. \tag{4.18}$$

The vertex correction acquires the form with $\mathcal{O}(\epsilon)$ accuracy:

$$\delta_{1Q}^{v,c} = g^2(-ia_\Gamma)\left\{C_F\left(-\frac{(-k_\perp^2)^\epsilon}{\epsilon^2} + \frac{(-q_{2\perp}^2)^\epsilon}{\epsilon} + \frac{\pi^2}{6} - 4 + \right.\right.$$

$$\left. + \frac{3q_{1\perp}^2}{q_{1\perp}^2 - q_{2\perp}^2}\ln\left[\frac{q_{1\perp}^2}{q_{2\perp}^2}\right]\right) + N_c\left(\frac{(-q_{1\perp}^2)^\epsilon}{2\epsilon} + \frac{\pi^2}{6} + 3 - \frac{1}{2}\ln^2\left[\frac{q_{1\perp}^2}{q_{2\perp}^2}\right]\right) +$$

$$\left. + (C_F - N_c)\left(\frac{1}{2}\ln^2\left[\frac{q_{2\perp}^2}{k_\perp^2}\right] + 2\text{Li}_2\left[1 - \frac{q_{1\perp}^2}{q_{2\perp}^2}\right]\right)\right\}. \tag{4.19}$$

The correction to the term violating helicity has the form that is finite in the limit $\epsilon \to 0$:

$$\delta_{2Q} = g^2(-ia_\Gamma)\left\{(N_c - C_F)\left(1 + \frac{k_\perp^2}{q_{1\perp}^2 - q_{2\perp}^2} - \frac{q_{1\perp}^2 k_\perp^2}{(q_{1\perp}^2 - q_{2\perp}^2)^2}\ln\left[\frac{q_{1\perp}^2}{q_{2\perp}^2}\right]\right) + \right.$$

$$\left. + C_F\frac{3\,q_{1\perp}^2}{q_{1\perp}^2 - q_{2\perp}^2}\ln\left[\frac{q_{1\perp}^2}{q_{2\perp}^2}\right]\right\} + \mathcal{O}(\epsilon). \tag{4.20}$$

For $\mathcal{N} = 4$ SYM case (all particles of the theory are in the adjoint color representation) one can obtain very simple result for the vertex:

$$\gamma_{R_1 Q_2}^{Q(SYM)} = -\frac{g}{k_3^+}\bar{u}(k_3)T_{QQ_2}^{R_1}\left\{\slashed{q}_{1\perp} + g^2 N_c(-ia_\Gamma)\left(\slashed{q}_{1\perp}\left[\frac{3}{2\epsilon}\left((-q_{1\perp}^2)^\epsilon + (-q_{2\perp}^2)^\epsilon\right) - \right.\right.\right.$$

$$\left.\left.\left. - \frac{(-k_\perp^2)^\epsilon}{\epsilon^2} - \frac{7}{2} + \frac{\pi^2}{3} - \frac{1}{2}\ln^2\frac{q_{1\perp}^2}{q_{2\perp}^2}\right] + (\slashed{q}_{1\perp} + \slashed{q}_{2\perp})\frac{3q_{1\perp}^2}{q_{1\perp}^2 - q_{2\perp}^2}\ln\frac{q_{1\perp}^2}{q_{2\perp}^2}\right)\right\}. \tag{4.21}$$

Here we have used the following substitutions: $C_F \to N_c$, $\frac{n_f}{N_c} \to 4$, $n_s \to 6 - 2\epsilon$ (in the dimensional reduction scheme).

5   Conclusion

Our paper is devoted to the effective vertex $\gamma^{Q}_{R_1 Q_2}$ calculation in the next-to-leading order. The vertex of the massless quark Q production in Reggeon (quark Q_2 and gluon R_1) collision in t-channels was the last unknown NLO vertex in the central rapidity region to formulate the quark Reggeization hypothesis within the next-to-leading logarithmic approximation. Now all components are ready to perform the hypothesis proof by the bootstrap approach [7] having been used in the gluon Reggeization proof both in QCD [10, 11, 12] and SYM [13]. The simplicity of the SYM vertex (4.21) gives us an additional tool for the SYM property investigations by use of multi-Regge amplitude form as it was the case for the gluon Reggeization and BDS anzats [24] in SYM.

In principle, there are some different methods of the effective vertex calculation with t-channel unitarity method being the most popular among them. However in our work we use the straightforward method of one-loop amplitude calculation having equipped with the computer algebra automatization methods based on the Mathematica system and "LiteRed" package (by R. N. Lee) [15] for it. This package is used to reduce integrals emerging in the one-loop amplitude to the basis of master integrals. Master integrals in our problem are of known (massless) pentagon and box types [14]. Our method allows us to perform the cross-check by obtaining another elements of the Regge amplitude (quark and gluon trajectories and known effective vertices) as a by-effect.

6 Appendix

6.1 Integrals calculation. Notation

We reduce all expressions for diagrams in Fig. 2 to scalar products and basic helicity structures. There are two vectors that are not included in the denominators of the pentagon diagram type in the amplitude. It means that there will be tensor integrals with up to two indices. There is only one topology of the integral in our problem:

$$J_{12345}(n_1, n_2, n_3, n_4, n_5) = J_{12345}(\vec{n}) = \int \frac{d^D l}{(2\pi)^D} \frac{1}{D_1^{n_1} D_2^{n_2} D_3^{n_3} D_4^{n_4} D_5^{n_5}}\,, \tag{6.1}$$

$$D_1 = l^2\,,\ D_2 = (l + k_1)^2\,,\ D_3 = (l + k_1 + k_2)^2\,,\ D_4 = (l + k_1 + k_2 + k_3)^2\,,$$
$$D_5 = (l + k_1 + k_2 + k_3 + k_4)^2.$$

There are only ten master integrals in this topology that have the form $J_{12345}(\vec{n}_i)\,,\ i = 1,\ldots,10$, where $\vec{n}_i$ are of the form:

$$\vec{n}_1 = (1,1,1,1,1)\,,\ \vec{n}_2 = (1,1,1,1,0)\,,\ \vec{n}_3 = (1,1,1,0,1)\,,\ \vec{n}_4 = (1,1,0,1,1)\,,$$
$$\vec{n}_5 = (1,0,1,1,1)\,, \vec{n}_6 = (1,0,1,0,0)\,,\ \vec{n}_7 = (1,0,0,1,0)\,,$$
$$\vec{n}_8 = (0,1,0,1,0)\,,\ \vec{n}_9 = (0,1,0,0,1)\,,\ \vec{n}_{10} = (0,0,1,0,1)\,,$$

and one has four integral types with the same topology with them having different permutations of the external momenta:

	D_1	D_2	D_3	D_4	D_5
J_{12345}	l^2	$(l+k_1)^2$	$(l+k_1+k_2)^2$	$(l+k_1+k_2+k_3)^2$	$(l+k_1+k_2+k_3+k_4)^2$
J_{21345}	l^2	$(l+k_2)^2$	$(l+k_1+k_2)^2$	$(l+k_1+k_2+k_3)^2$	$(l+k_1+k_2+k_3+k_4)^2$
J_{12435}	l^2	$(l+k_1)^2$	$(l+k_1+k_2)^2$	$(l+k_1+k_2+k_4)^2$	$(l+k_1+k_2+k_3+k_4)^2$
J_{41235}	l^2	$(l+k_4)^2$	$(l+k_1+k_4)^2$	$(l+k_1+k_2+k_4)^2$	$(l+k_1+k_2+k_3+k_4)^2$

There are only three types of different master integrals. The first one is a pentagon with massless external lines (for example, $J_{12345}(\vec{n}_1)$). The second one is a box with one external line with mass (for example, $J_{12345}(\vec{n}_2)$). And the third type is a bubble (for example, $J_{12345}(\vec{n}_6)$).

The following table shows the integrals used in the diagrams in Fig. 2:

Integrals	Diagrams
J_{12345}	d5, d4.1, d4.2, d4.4, d3.X, d2.X
J_{21345}	d5c, d4.1c, d4.2c
J_{12435}	d4.3
J_{41235}	d4.3c

6.2 Tensor momentum integrals

We introduce the following notation $I[.]$ for various integrands containing the argument of the square bracket. For instance,

$$I\left[l^{\mu}\right] \equiv \int \frac{d^D l}{(2\pi)^D} \frac{l^{\mu}}{D_1^{n_1} D_2^{n_2} D_3^{n_3} D_4^{n_4} D_5^{n_5}} \tag{6.2}$$

Integral with an external index μ is expressed as a linear combination of the incoming momenta:

$$I\left[l^{\mu}\right] = \sum_i k_i^{\mu} I[a_i], \tag{6.3}$$

where a_i are scalar polynomial functions of l^{μ}. It is easy to express the integral with an external index as a linear combination of integrals without external indices. Since we have four independent vectors k_i (that are in the four-dimensional subspace), so the matrix m_{ij} is invertible. It is easy to find that eventually

$$I\left[l^{\mu}\right] = \sum_{ij} k_i^{\mu} m_{ij}^{-1} I\left[(k_j, l)\right], \ (k_i, k_j) = m_{ij}, \tag{6.4}$$

where $I\left[(k_j, l)\right]$ is expressed in terms of integrals with reduced powers of denominators.

Tensor integral with two indices is expressed through the metric tensor subspace $D - 4$, and entering into integral momenta

$$I\left[l^{\mu} l^{\nu}\right] = g_{D-4}^{\mu\nu} I[A] + \sum_{i,j,r,n} m_{ij}^{-1} m_{rn}^{-1} k_i^{\mu} k_r^{\nu} I\left[(k_j, l)(k_n, l)\right], \tag{6.5}$$

$$g_{D-4}^{\mu\nu} k_{i\mu} = 0, \ g_{D-4}^{\mu\nu} g_{\mu\nu} = D - 4.$$

The coefficient before the metric tensor can be easily calculated:

$$I[A] = \frac{1}{D-4}\left(I\left[l^2\right] - \sum_{ij} m_{ij}^{-1} I\left[(l, k_i)(l, k_j)\right]\right), \tag{6.6}$$

$$I[l^{\mu} l^{\nu}] = \frac{g^{\mu\nu} - m_{ij}^{-1} k_i^{\mu} k_j^{\nu}}{D-4}\left(I[l^2] - m_{rn}^{-1} I[(l, k_r)(l, k_n)]\right) + $$
$$+ m_{ij}^{-1} m_{rn}^{-1} k_i^{\mu} k_r^{\nu} I[(k_j, l)(k_n, l)] \tag{6.7}$$

The integrals with three external Lorentz indices will not arise in our problem. A loop momentum convoluted with the momentum included in the denominator is easily expressed in terms of a linear combination of the denominators. Integrals with two indices appear only in the expression of $I[(e, l)l]$.

6.3 Master Integrals

We work in the dimensional regularization with $D = 4 + 2\epsilon$. Hereafter we use the notation for the common multiplier emerging in integral calculations.

$$a_\Gamma = i\frac{\Gamma\left(3 - \frac{D}{2}\right)\Gamma^2\left(\frac{D}{2} - 1\right)}{(4\pi)^{\frac{D}{2}}\Gamma(D - 3)}. \tag{6.8}$$

In the master integral expressions [14] we assume all the invariants to be negative. To continue analytically these expressions to the physical region of our process (See Fig 1) it is necessary to make a prescription $(k_i + k_j)^2 = s_{ij} \to s_{ij} + i0$ for the invariants involved.

There are three principal master integrals in our calculation [14]:

$$J_{12345}(1, 0, 1, 0, 0) = \int \frac{d^D l}{(2\pi)^D} \frac{1}{l^2(l + k_1 + k_2)^2} = -a_\Gamma \frac{(-t_1)^\epsilon}{\epsilon(1 + 2\epsilon)}, \ t_1 < 0;$$

$$J_{12345}(1, 1, 1, 1, 0) = \int \frac{d^D l}{(2\pi)^D} \frac{1}{l^2(l + k_1)^2(l + k_1 + k_2)^2(l + k_1 + k_2 + k_3)^2} =$$

$$= 2a_\Gamma \frac{(-t_2)^{-\epsilon}}{(-t_1)^{1-\epsilon}(-s_1)^{1-\epsilon}}\left[\frac{1}{\epsilon^2} + \text{Li}_2\left(1 - \frac{t_1}{t_2}\right) + \text{Li}_2\left(1 - \frac{s_1}{t_2}\right) - \frac{\pi^2}{6}\right] + \mathcal{O}(\epsilon),$$

$s_1 < 0, \ t_1 < 0, \ t_2 < 0;$

$$J_{12345}(1, 1, 1, 1, 1) =$$

$$= \int \frac{d^D l}{(2\pi)^D} \frac{1}{l^2(l + k_1)^2(l + k_1 + k_2)^2(l + k_1 + k_2 + k_3)^2(l + k_1 + k_2 + k_3 + k_4)^2} =$$

$$= -a_\Gamma\left\{\frac{(-s)^{-\epsilon}(-t_1)^{-\epsilon}}{(-s_1)^{1-\epsilon}(-s_2)^{1-\epsilon}(-t_2)^{1-\epsilon}}\left(\frac{1}{\epsilon^2} + 2\text{Li}_2\left(1 - \frac{s_1}{s}\right) + 2\text{Li}_2\left(1 - \frac{t_2}{t_1}\right) - \frac{\pi^2}{6}\right) + \right.$$

$$+ \frac{(-t_1)^{-\epsilon}(-s_1)^{-\epsilon}}{(-s_2)^{1-\epsilon}(-t_2)^{1-\epsilon}(-s)^{1-\epsilon}}\left(\frac{1}{\epsilon^2} + 2\text{Li}_2\left(1 - \frac{s_2}{t_1}\right) + 2\text{Li}_2\left(1 - \frac{s}{s_1}\right) - \frac{\pi^2}{6}\right) +$$

$$+ \frac{(-s_1)^{-\epsilon}(-s_2)^{-\epsilon}}{(-t_2)^{1-\epsilon}(-s)^{1-\epsilon}(-t_1)^{1-\epsilon}}\left(\frac{1}{\epsilon^2} + 2\text{Li}_2\left(1 - \frac{t_2}{s_1}\right) + 2\text{Li}_2\left(1 - \frac{t_1}{s_2}\right) - \frac{\pi^2}{6}\right) +$$

$$+ \frac{(-s_2)^{-\epsilon}(-t_2)^{-\epsilon}}{(-s)^{1-\epsilon}(-t_1)^{1-\epsilon}(-s_1)^{1-\epsilon}}\left(\frac{1}{\epsilon^2} + 2\text{Li}_2\left(1 - \frac{s}{s_2}\right) + 2\text{Li}_2\left(1 - \frac{s_1}{t_2}\right) - \frac{\pi^2}{6}\right) +$$

$$+ \frac{(-t_2)^{-\epsilon}(-s)^{-\epsilon}}{(-t_1)^{1-\epsilon}(-s_1)^{1-\epsilon}(-s_2)^{1-\epsilon}}\left(\frac{1}{\epsilon^2} + 2\text{Li}_2\left(1 - \frac{t_1}{t_2}\right) + 2\text{Li}_2\left(1 - \frac{s_2}{s}\right) - \frac{\pi^2}{6}\right)\right\} + \mathcal{O}(\epsilon),$$

$s < 0, \ s_1 < 0, \ s_2 < 0, \ t_1 < 0, \ t_2 < 0;$

23

Here we use notations (2.1) for kinematic invariants.

In the analytical continuation to the physical domain in polylogarithmic functions one needs to choose the correct branch using the following properties:

$$\mathrm{Li}_2(x \pm i0) = \frac{\pi^2}{3} - \frac{1}{2}\ln^2 x - \mathrm{Li}_2(x^{-1}) \pm i\pi \ln x , \quad x > 1$$

Providing σ_1, σ_2 to be the signs of s_1, s_2, for the case $\sigma_1\sigma_2 = -1$ one has

$$\mathrm{Li}_2\left(1 - \frac{s_1 + i0}{s_2 + i0}\right) = \frac{\pi^2}{3} - \frac{1}{2}\ln^2\left(1 - \frac{s_1}{s_2}\right) - \mathrm{Li}_2\left(\frac{1}{1 - \frac{s_1}{s_2}}\right) + i\sigma_1\pi \ln\left(1 - \frac{s_1}{s_2}\right).$$

References

[1] I. I. Balitsky and L. N. Lipatov, Sov. J. Nucl. Phys. **28** (1978) 822 [Yad. Fiz. **28** (1978) 1597].

[2] V. S. Fadin, E. A. Kuraev and L. N. Lipatov, Phys. Lett. B **60** (1975) 50.

[3] E. A. Kuraev, L. N. Lipatov and V. S. Fadin, Zh. Eksp. Teor. Fiz. **71** (1976) 840 [Sov. Phys. JETP **44** (1976) 443].

[4] E. A. Kuraev, L. N. Lipatov and V. S. Fadin, Zh. Eksp. Teor. Fiz. **72** (1977) 377 [Sov. Phys. JETP **45** (1977) 199].

[5] L. N. Lipatov, Sov. J. Nucl. Phys. **23**, 338 (1976).

[6] A. V. Bogdan, A. V. Grabovsky, Nucl. Phys. B773 (2007) 65–83.

[7] V. S. Fadin, R. Fiore, M. G. Kozlov, and A. V. Reznichenko, Phys. Lett. B **639** (2006) 74 [arXiv:hep-ph/0602006].

[8] A. V. Bogdan and V. S. Fadin, Nucl. Phys. B 740 (2006) 36–57.

[9] V. S. Fadin, M. G. Kozlov and A. V. Reznichenko, Yad. Fiz. **67**, 377 (2004) [Phys. Atom. Nucl. **67**, 359 (2004)], [hep-ph/0302224].

[10] V. S. Fadin, M. G. Kozlov, A. V. Reznichenko, Phys.Atom.Nucl. vol. **74**, (2011) pp. 758-770 [Preprint INP 2010-26].

[11] V. S. Fadin, M. G. Kozlov, and A. V. Reznichenko, Phys.Atom.Nucl. vol. **75**, (2012), pp. 850-865 [Preprint INP 2011-23].

[12] V. S. Fadin, M. G. Kozlov, and A. V. Reznichenko, Phys.Atom.Nucl., vol. **75**, (2012) pp. 493-506 [Preprint INP 2011-24].

[13] V. S. Fadin, M. G. Kozlov, A. V. Reznichenko, Phys.Atom.Nucl., vol. **77** (2014), pp. 251-273 [Preprint INP 2012-32].

[14] Z. Bern, L. Dixon, and D. Kosower, Nucl.Phys. B **412** (1994) pp. 751-816 [SLAC-PUB-5947, hep-ph/9306240].

[15] R. N. Lee, arXiv:1212.2685 (2012).

[16] V. S. Fadin, R. Fiore, Phys.Rev. D64 (2001) 114012

[17] L. N. Lipatov and M. I. Vyazovsky, Nucl. Phys. B 597 (2001), 399, arXiv:hep-ph/0009340

[18] V. S. Fadin, Phys. Atom. Nucl. 66, 2017 (2003).

[19] R. E. Gerasimov, V. S. Fadin, Phys.Atom. Nucl. 73 (2010) 1214–1228, Preprint INP 2008-36.

[20] A.V. Bogdan, A.V. Grabovsky,Nucl.Phys. B 757 (2006), 211-232

[21] V. S. Fadin and L.N. Lipatov, Nucl. Phys. B 406 (1993), 259–292

[22] V. S. Fadin, R. Fiore and A. Papa, Phys. Rev. D 63 (2001), 034001, arXiv:hep-ph/008006

[23] V. Del Duca and C. R. Schmidt, Phys. Rev. D 59 (1999), 074004

[24] Z. Bern, L. J. Dixon and V. A. Smirnov, Phys. Rev. D **72** (2005) 085001 [hep-th/0505205].

M.G. Kozlov, A.V. Reznichenko

Effective vertex of quark production
in collision of Reggeized quark and gluon

Budker INP 2015-10